Supporting Information

The Novel Dual-Category Active Sites of NiCoP/CoP as High-performance Electrocatalyst for Urea Electrolysis and Synergistic Hydrogen Production

Borong Lu, Dong Wang, Chunlin Zhao, Kai Zhu, Jun Yan, Guiling Wang, Dianxue Cao, Ke Ye*

Key Laboratory of Superlight Materials and Surface Technology of Ministry of Education, College of Materials Science and Chemical Engineering, Harbin Engineering University, Harbin 150001, China.

* Corresponding author.

E-mail address: yekehrbeu@163.com

Experimental Section

Chemicals and Materials

All chemical reagents are analytically pure and can be used directly without further purification, including Ni foam (NF), deionized water (H_2O), potassium hydroxide (KOH), urea ($CO(NH_2)_2$), methyl alcohol (CH_3OH), nickel nitrate hexahydrate ($Ni(NO_3)_2·6H_2O$), 2-methylimidazole ($C_4H_6N_2$), cobalt nitrate hexahydrate ($Co(NO_3)_2·6H_2O$). In addition, Ni foam (NF) was used after sonication for 15 min in acetone, methanol, and deionized water, respectively. Then, it was cleaned with DI water and absolute ethanol.

Synthesis of NiCo-LDH/NF

Typically, $Ni(NO_3)_2·6H_2O$ (0.462 g), $Co(NO_3)_2·6H_2O$ (0.22 g), and $CO(NH_2)_2$ (0.72 g) were dispersed into deionized water (35 mL) and stirred for 30 min. Then, the above solution and pretreated NF (1 cm × 4 cm) were transferred to a 50 mL Teflon-lined autoclave and heated at 120 °C for 8 h. The autoclave was slowly cooled to room temperature. After washing several times with deionized water and ethanol. The resulting catalyst was dried at 80 °C for 6 h, the drying NiCo-LDH/NF was obtained.

Synthesis of NiCo-LDH/ZIF-67

The NiCo-LDH/ZIF-67 was synthesized by a one-step synthesis method at normal temperature. Typically, solution A: 2-methylimidazole (0.8 g), and solution B: $Co(NO_3)_2·6H_2O$ (0.291 g) were dispersed into methyl alcohol (20 mL), respectively. After stirring for 15 min, solutions A and B were mixed for 15 min. Subsequently, the

NiCo-LDH/NF was tilted into the mixture solution and resting for 24 h at room temperature. After washing several times with methyl alcohol. The NiCo-LDH/ZIF-67 was dried at 80 °C for 6 h.

Synthesis of CNCP-T (200, 300, 350, 400)

A porcelain boat containing 300 mg of sodium hypophosphite was placed upstream of the tube furnace, and the downstream was NiCo-LDH/ZIF-67. Then the tube furnace was heated at 200, 300, 350, and 400 °C in the argon atmosphere for 2 h with a heating rate of 2 °C min^{-1} to synthesize CNCP-200, CNCP-300, CNCP-350, and CNCP-400.

Synthesis of CoP

As a controlled sample, ZIF-67 was grown directly on bare NF, and then put into a tube furnace and heated in an argon atmosphere at 350°C for 2 h at a heating rate of 2°C min^{-1} for synthesis.

Synthesis of NiCoP

The synthesis process of NiCoP is similar to that of CoP, but using NiCo-LDH in the precursor solution.

Physical Characterizations

X-ray diffraction (XRD) patterns were obtained from a Rigaku TTR III with Cu Kα radiation. Scanning electron microscopy (SEM) images were recorded by a JEOL JSM-6480A. The high-resolution transmission electron microscope (HRTEM) and scanning TEM (STEM)-EDS analysis were acquired from a Tecnai G2 F20 S-TWIN. X-ray

photoelectron spectroscopy (XPS) was performed on a Thermo ESCALAB 250.

Electrochemical measurements

The electrochemical measurements were performed on an Ivium electrochemical workstation (Ivium-n-Stat, Holland) with a three-electrode system. The CNCP-T, NiCo-LDH/ZIF-67, and NiCo-LDH as the working electrode, Ag/AgCl (saturated KCl), and graphite rod were used as the reference and counter electrodes, respectively. If not specifically mentioned, UOR tests were carried out in N_2-saturated 1 M KOH with 0.5 M urea electrolyte, and HER tests were carried out in N_2-saturated 1 M KOH, respectively. All potentials measured were calculated relative to versus reversible hydrogen electrode (RHE) and calculated using the formula: E(RHE) = E(Ag/AgCl) + 0.197+ 0.0592 pH. The Tafel plots were derived from the Tafel equation $\eta = b\log j + \alpha$ (where η is the overpotential, b is the Tafel slope, j is the current density).

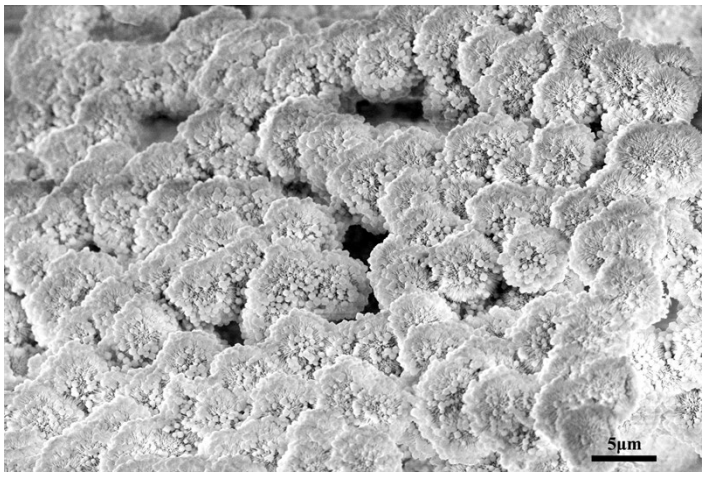

Figure S1. The SEM image of CNCP-350.

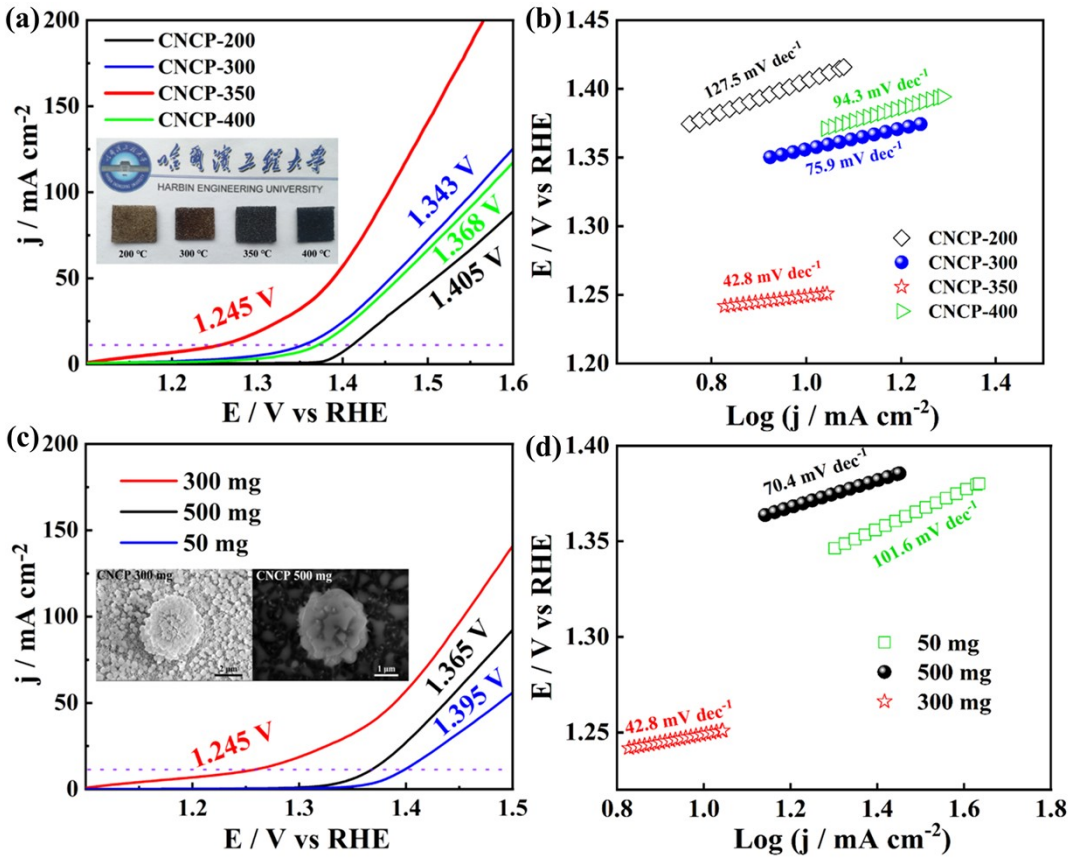

Figure S2. (a) The LSV curves of CNCP-T in the 1.0 M KOH + 0.5 M urea. (b) Tafel plots of the CNCP-T. (c) The LSV curves of CNCP-350 with different phosphating amounts in the 1.0 M KOH + 0.5 M urea. (d) Tafel plots of the CNCP-350 with different phosphating amounts.

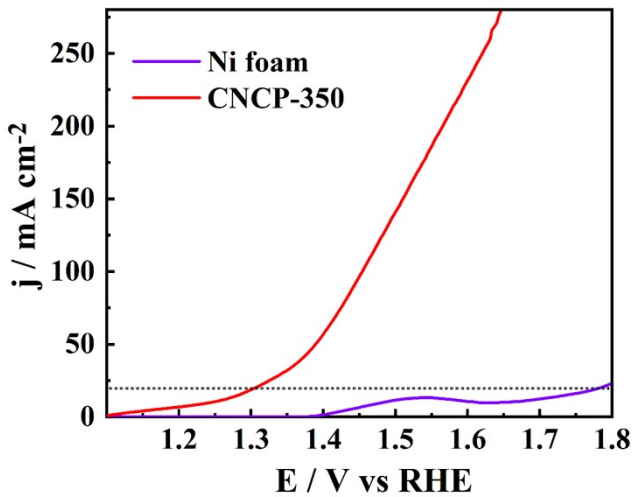

Figure S3. LSV curves of CNCP-350 and NF in 1 M KOH + 0.5 M urea electrolyte.

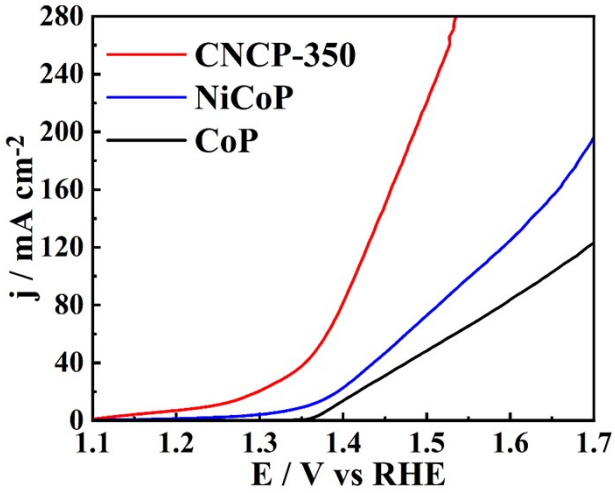

Figure S4. The LSV curves of NiCoP, CoP, and CNCP-350 in 1.0 M KOH + 0.5 M urea.

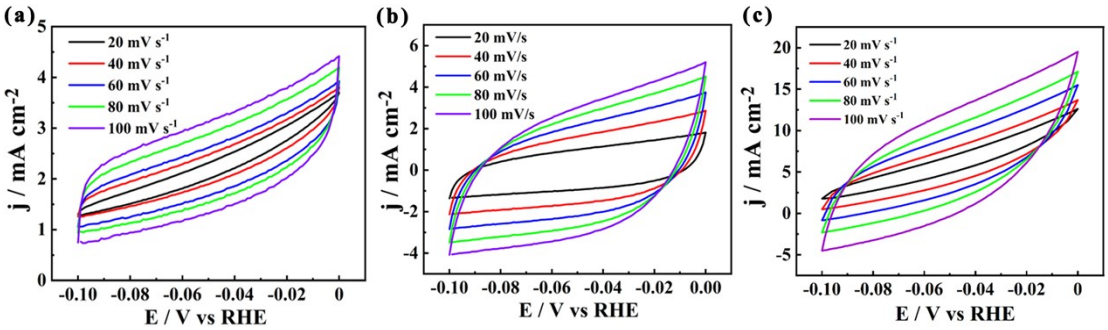

Figure S5. (a-c) UOR: the CV curve of the NiCo-LDH, NiCo-LDH/ZIF-67 and CNCP-350 (20-100 mV s^{-1}).

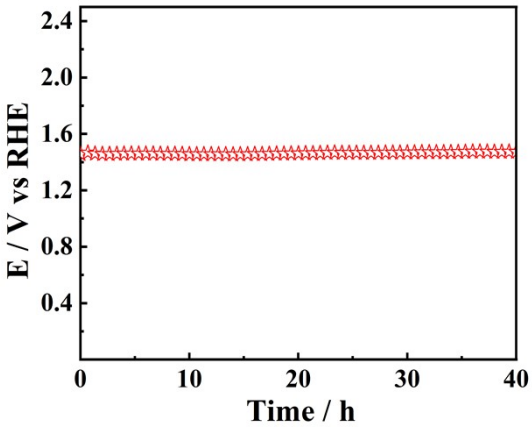

Figure S6. The chronoamperometric response of CNCP-350 in 1.0 M KOH + 0.5 M urea at 100 mA cm^{-2} for 40 h (UOR).

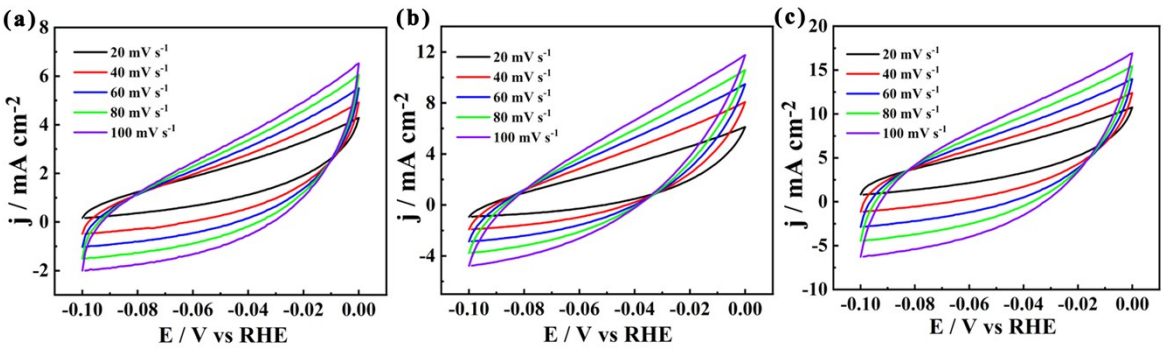

Figure S7. (a-c) HER: the CV curve of the NiCo-LDH, NiCo-LDH/ZIF-67 and CNCP-350 (20-100 mV s^{-1}).

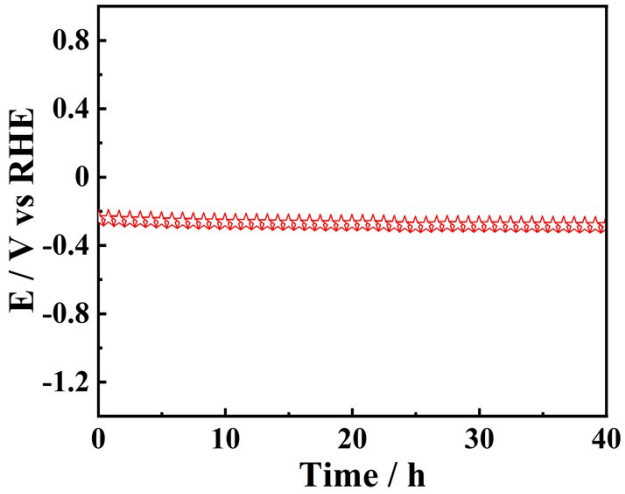

Figure S8. The chronoamperometric response of CNCP-350 in 1.0 M KOH + 0.5 M urea at 100 mA cm^{-2} for 40 h (HER).

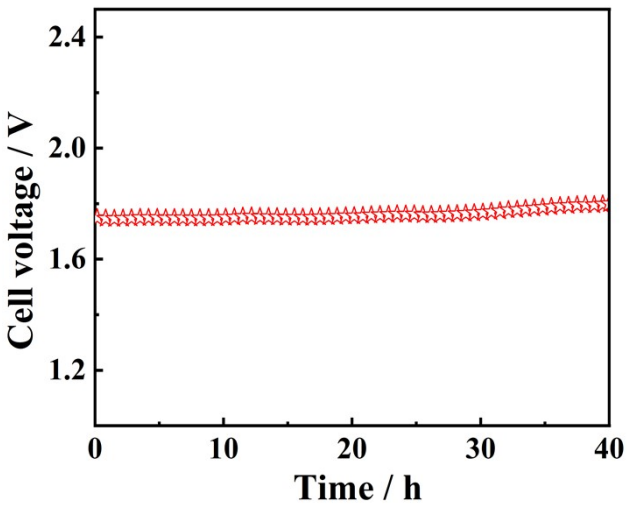

Figure S9. The chronoamperometric response of CNCP-350 in 1.0 M KOH + 0.5 M urea at 100 mA cm^{-2} for 40 h (HER‖UOR).

Table S1. Comparison of the UOR activity of the CNCP-350 and several recently reported catalysts.

Materials	Electrolyte	Potential (V)	Current density (mA cm^{-2})	Reference
$FeNi_3$-MoO_2	1.0 M KOH+0.5 M urea	1.290 V	10 mA cm^{-2}	1
Ni-NiO-$Mo_{0.84}Ni_{0.16}$	1.0 M KOH+0.5 M urea	1.330 V	50 mA cm^{-2}	2
Ni_3S_2/Ni	1.0 M KOH+0.5 M urea	1.300 V	10 mA cm^{-2}	3
Ni_3S_2–Ni_3P	1.0 M KOH+0.5 M urea	1.379 V	100 mA cm^{-2}	4
C-350	1.0 M KOH+0.5 M urea	1.337 V	10 mA cm^{-2}	5
$NiFe(OH)_x/Ni_3N$	1.0 M KOH+1 M urea	1.360 V	10 mA cm^{-2}	6
Ni-S-Se	1.0 M KOH+0.5 M urea	1.380 V	10 mA cm^{-2}	7
O-NiMoP	1.0 M KOH+0.5 M urea	1.410 V	100 mA cm^{-2}	8
$NiCo_2S_4$ NS	1.0 M KOH+0.5 M urea	1.272 V	10 mA cm^{-2}	9
CNCP-350	1.0 M KOH+0.5 M urea	1.245 V	10 mA cm^{-2}	This work

Table S2. Impedance fitting data of the CNCP-350, NiCo-LDH/ZIF-67 and NiCo-LDH.

Materials	R_s(Ω)	R_{ct}(Ω)
NiCo-LDH	0.625	0.667
NiCo-LDH/ZIF-67	0.621	0.488

CNCP-350	0.619	0.393

Table S3. Comparison of the HER activity of the CNCP-350 and several recently reported catalysts.

Materials	Electrolyte	Overpotential (mV)	Current density (mA cm^{-2})	Reference
Ni_3S_2−Ni_3P/NF-2	1.0 M KOH	122 mV	10 mA cm^{-2}	4
Ni-S-Se/NF	1.0 M KOH	98 mV	10 mA cm^{-2}	7
Co−Ni−P-2	1.0 M KOH	103 mV	10 mA cm^{-2}	10
Cu@NC NT/CF	1.0 M KOH	123 mV	10 mA cm^{-2}	11
$Co_zW_yS_x$	1.0 M KOH	189 mV	10 mA cm^{-2}	12
NiTe/rGO/NF	1.0 M KOH	170 mV	10 mA cm^{-2}	13
Co_xMo_yS-CC	1.0 M KOH	85 mV	10 mA cm^{-2}	14
MNPBA-P	1.0 M KOH	134 mV	10 mA cm^{-2}	15
Ni_3N/NF	1.0 M KOH	120 mV	10 mA cm^{-2}	16
CNCP-350	1.0 M KOH	65 mV	10 mA cm^{-2}	This work

Table S4. Comparison of the dual-electrode UOR activity of the CNCP-350 and several recently reported catalysts.

Materials	Electrolyte	Potential (V)	Current density (mA cm^{-2})	Reference
$FeNi_3$-MoO_2	1.0 M KOH+0.5 M urea	1.370 V	10 mA cm^{-2}	1
Ni-NiO-	1.0 M KOH+0.5	1.370 V	10 mA cm^{-2}	2

$Mo_{0.84}Ni_{0.16}$	M urea			
Ni_3S_2/Ni	1.0 M KOH+0.5 M urea	1.360 V	10 mA cm^{-2}	3
Ni_3S_2–Ni_3P	1.0 M KOH+0.5 M urea	1.430 V	10 mA cm^{-2}	4
Ni_3N	1.0 M KOH+0.5 M urea	1.370 V	10 mA cm^{-2}	16
MNPBA-P	1.0 M KOH+1 M urea	1.500 V	10 mA cm^{-2}	15
Ni-S-Se	1.0 M KOH+0.5 M urea	1.470 V	10 mA cm^{-2}	7
O-NiMoP	1.0 M KOH+0.5 M urea	1.360 V	100 mA cm^{-2}	8
$NiCo_2S_4$ NS	1.0 M KOH+0.5 M urea	1.450 V	10 mA cm^{-2}	9
CNCP-350	1.0 M KOH+0.5 M urea	1.245 V	10 mA cm^{-2}	This work

References

[S1] Q. L. Xu, T. Q. Yu, J. L. Chen, G. F. Qian, H. N. Song, L. Luo, Y. L. Chen, T. Y. Liu, Y. Z. Wang, S. B. Yin, Coupling interface constructions of $FeNi_3$-MoO_2 heterostructures for efficient urea oxidation and hydrogen evolution reaction, ACS Appl. Mater. Interfaces., 13 (2021) 16355–16363.

[S2] Q. L. Xu, G. F. Qian, S. B. Yin, C. Yu, W. Chen, T. Q. Yu, L. Luo, Y. J. Xia, P. Tsiakaras, Design and synthesis of highly performing bifunctional Ni-NiO-MoNi hybrid catalysts for enhanced urea oxidation and hydrogen evolution reactions, ACS Sustainable Chem. Eng., 8 (2020) 7174–7181.

[S3] X. Y. Zhuo, W. J. Jiang, G. F. Qian, J. L. Chen, T. Q. Yu, L. Luo, L. H. Lu, Y. L.

Chen, S. B. Yin, Ni_3S_2/Ni heterostructure nanobelt arrays as bifunctional catalysts for urea-rich wastewater degradation., ACS Appl. Mater. Interfaces., 13 (2021) 35709–35718.

[S4] J. C. Liu, Y. Wang, Y. F. Liao, C. L. Wu, Y. G. Yan, H. J. Xie, Y. G. Chen, Heterostructured Ni_3S_2-Ni_3P/NF as a bifunctional catalyst for overall urea−water electrolysis for hydrogen generation, ACS Appl. Mater. Interfaces., 13 (2021) 26948–26959.

[S5] S. N. Hu, S. Q. Wang, C. Q. Feng, H. M. Wu, J. J. Zhang, H. Mei, Novel MOF-derived nickel nitride as high-performance bifunctional electrocatalysts for hydrogen evolution and urea oxidation, ACS Sustainable Chem. Eng., 8 (2020) 7414–7422.

[S6] H. J. Zhang, X. F. Meng, J. F. Zhang, Y. Huang, Hierarchical NiFe hydroxide/Ni_3N nanosheet-on-nanosheet heterostructures for bifunctional oxygen evolution and urea oxidation reactions, ACS Sustainable Chem. Eng., 9 (2021) 12584–12590.

[S7] N. Chen, Y. K. Du, G. Zhang, W. T. Lu, F. F. Cao, Amorphous nickel sulfoselenide for efficient electrochemical urea-assisted hydrogen production in alkaline media, Nano Energy, 81 (2021) 105605.

[S8] H. Jiang, M. Z. Sun, S. L. Wu, B. L. Huang, C. S. Lee, W. J. Zhang, Oxygen-incorporated NiMoP nanotube arrays as effcient bifunctional electrocatalysts for urea-assisted energy-saving hydrogen production in alkaline electrolyte, Adv. Funct. Mater., 31 (2021) 2104951.

[S9] W. X. Zhu, M. R. Ren, N. Hu, W. T. Zhang, Z. T. Luo, R. Wang, J. Wang, L. J. Huang, Y. R. Suo, J. L. Wang, Traditional $NiCo_2S_4$ phase with porous nanosheets array topology on carbon cloth: a flexible, versatile and fabulous electrocatalyst for overall water and urea electrolysis, ACS Sustainable Chem. Eng., 6 (2018) 5011–5020.

[S10] Y. Pei, Y. Yang, F. Zhang, P. Dong, R. Baines, Y. Ge, H. Chu, P. M. Ajayan, J. Shen, M. Ye, Controlled electrodeposition synthesis of Co-Ni-P film as a flexible and inexpensive electrode for efficient overall water splitting, ACS Appl. Mater.

Interfaces., 9 (2017) 31887–31896.

[S11] Y. Zhang, Y. Ma, Y. Y. Chen, L. Zhao, L. B. Huang, H. Luo, W. J. Jiang, X. Zhang, S. Niu, D. Gao, J. Bi, G. Fan, J. S. Hu, Encased copper boosts the electrocatalytic activity of N-doped carbon nanotubes for hydrogen evolution, ACS Appl. Mater. Interfaces., 9 (2017) 36857–36864.

[S12] K. Fan, H. Zou, N. V. R. A. Dharanipragada, L. Fan, A. K. Inge, L. Duan, B. Zhang, L. Sun, Surface and bulk reconstruction of CoW sulfides during ph-universal electrocatalytic hydrogen evolution, J. Mater. Chem. A., 9 (2021) 11359–11369.

[S13] Z. Wang, P. Guo, M. Liu, C. Guo, H. Liu, S. Wei, J. Zhang, X. Lu, Rational design of metallic NiTex (x = 1 or 2) as bifunctional electrocatalysts for efficient urea conversion, ACS Appl Energ Mater., 2 (2019) 3363–3372.

[S14] P. Li, Z. Zhuang, C. Du, D. Xiang, F. Zheng, Z. Zhang, Z. Fang, J. Guo, S. Zhu, W. Chen, Insights into the Mo-Doping effect on the electrocatalytic performance of hierarchical CoxMoyS nanosheet arrays for hydrogen generation and urea oxidation, ACS Appl. Mater. Interfaces., 12 (2020) 40194–40203.

[S15] H. Xu, K. Ye, K. Zhu, Y. Gao, J. Yin, J. Yan, G. Wang, D. Cao, Transforming carnation-shaped MOF-Ni to Ni–Fe prussian blue analogue derived efficient bifunctional electrocatalyst for urea electrolysis, ACS Sustainable Chem. Eng., 8 (2020) 16037–16045.

[S16] S. Hu, C. Feng, S. Wang, J. Liu, H. Wu, L. Zhang, J. Zhang, Ni_3N/NF as bifunctional catalysts for both hydrogen generation and urea decomposition, ACS Appl. Mater. Interfaces., 11 (2019) 13168–13175.